ISSN 1392-1207. MECHANIKA. Vol. 29, No. 4, 2023: 309–316

Tuning of Mixing Zone Parameters in a Dynamic Mixer and Performance Comparison with Screw-Based Mixers

Jiagang SUN*, Jiankang WANG, Yiwen ZHENG***, Zhijun LI******

**Tianjin Key Laboratory of Integrated Design and On-line Monitoring for Light Industry & Food Machinery and Equipment, Tianjin International Joint Research and Development Center of Low-carbon Green Process Equipment, School of Mechanical Engineering, Tianjin University of Science and Technology, Tianjin 300222, China; E-mail: sunjiagang@tust.edu.cn*

***Tianjin Key Laboratory of Integrated Design and On-line Monitoring for Light Industry & Food Machinery and Equipment, Tianjin International Joint Research and Development Center of Low-carbon Green Process Equipment, College of Mechanical Engineering, Tianjin University of Science and Technology, Tianjin 300222, China; E-mail: wangjk@tust.edu.cn (Corresponding author)*

****School of Mechanical Engineering, Tianjin University of Science and Technology, Tianjin 300222, China; E-mail: 503631057@qq.com*

*****School of Mechanical Engineering, Tianjin University of Science and Technology, Tianjin 300222, China; E-mail: lizj1224@163.com*

https://doi.org/10.5755/j02.mech.33213

1. Introduction

In polymer processing field, mixing is a necessary process for obtaining uniform mass distribution and temperature distribution, and then getting good performance. Usually, it is performed by the screw [1, 2], dynamic mixer [3] and static mixer [4].

In the past years, researches have been working on the mixing mechanism, aiming to improve the melt mixing quality. Robinson and Cleary [5] used the Lagrangian method to investigate the effects of screw pitch, knead block stagger angle, gap size, and filling level on the mixing behaviors, hence founding that the mixing rate was positively correlated to the screw pitch and gap size, and the largest mixing rate was obtained with the block angle of 30º, and the filling level of 50%. Cai et al. [6] investigated the mixing quality of the double-screw conical mixer, and produced best result and the lowest power consumption after choosing the particle diameter and rotation ratio. Belhout C. et al. [7] used numerical method to investigate the effects of Reynolds number, viscosity, aspect ratio and the number of mixing elements on the flow patterns and pressure drop of melt in static mixer. They found that the viscosity and Reynolds number, verified by similar experimental results, were two important factors influencing the performances of static mixers, and their results were similar to and verified by the experimental results. Huo et al. [8] found the reduction of rotational speed and filling level of screw mixer could increase the mixing rate. Connelly et al. [9] used the segregation scale (S) to characterize the melt mixing quality. The separation scale characterises the mixing process, with smaller values indicating uniform mixing. They found at the initial stage, the twin screw mixer had uniform melt mixing quality than the single screw mixer, however after 10 revolutions their segregation scales were nearly equal to each other. The minimum segregation scale of 100 μm was observed in their results. More literature about mixing can be found [10].

Although a lot of research has been done to improve melt mixing quality, how to get the uniform melt mixing quality with less pressure consumption is still a remain ing issue. Talhaoui et al. [11] investigated the flow pattern and mixing behavior of fluid in newly-developed mixer, realizing that the improvement of melt mixing quality usually comes with the increase of pressure drop and the length of mixers. Marschik et al. [12] investigated the effects of geometrical parameters on the melt mixing quality, pressure consumption and energy dissipation of block-head mixer, and found the pressure consumption depends mainly on the number of flights at the same axial position. Their results also showed that the melt mixing quality had a positive correlation with the pressure consumption and energy dissipation.

In this study, a new type of dynamic mixer is designed to mix two polymer melts. Three selected structural parameters of mixing zone, are used to analyse their influences on S and pressure drop (Δp), and the most effective structure for the product of S and Δp is obtained by using Taguchi orthogonal arrays method. The effects of flow rate and rotational speed on S and Δp are investigated, followed by the comparison among the mixing properties of the dynamic mixer those of screw-based mixers and slotted-screw mixers.

2. Method and characterization

2.1. Geometry and grid

The dynamic mixer is mounted where two polymer melts converge, with an internal rotational cone-shape rotor driven by a servo motor, as shown in Fig. 1, a and b. The rotor has a skirt edge with the thickness of 2 mm, and there are $N \times M$ holes with diameter of d_3, evenly distributed on the skirt edge. The inner space of dynamic mixer includes entrance, mixing and exit zones. The melts can successively flow through all of them, after being combined in mixing zone.

Three main parameters N, M, and d_3 of mixing zone are optimized for the minimum product of S and Δp using Taguchi orthogonal arrays method, and their levels and values are showed in Table 1. The N is the number of circles of holes, valued as 1, 2 and 3, the corresponding height L_2 of the shirt edge is 3, 6, and 9 mm, and the corresponding length of mixing zone L_m is 18, 21 and 24 mm, respectively. The values of M are 14, 20 and 26, representing the numbers of holes per circle on the skirt edge. The values of d_3 are 1.5, 2 and 2.5 mm, representing the diameter of holes on the skirt edge.

The diameter D_i and length L_i of entrance zone are 16 and 8 mm, and the diameter D_o and lengths L_o of exit zone are 12 and 5 mm, respectively. The gap between the rotor and channel wall is 1 mm. Moreover, the other dimensions are directly marked in Fig. 1b. The four positions Pr1 to Pr4, located on inlet surface, junction between entrance and mixing zones, junction between mixing and exit zones, and outlet surface, respectively, are selected to observe the simulation results of dynamic mixer.

In order to compare mixing properties, the screw-based mixer and slotted-screw mixer with the same entrance and exit dimensions D_i, L_i, D_o and L_o are selected to mix melts, as shown in Fig. 1, c and d. The pitch of screw-based mixer is 16 mm, same to D_i. The gap between screw and channel wall is 0.8 mm. The thickness of screw-based flight is 2 mm. The L_m of screw mixer is equal to $Ns{\cdot}Di$+5 mm, where Ns is 5.

Table 1

Factor level

Level	Factor		
	N	M	d_3, mm
I	1	14	1.5
II	2	20	2
III	3	26	2.5

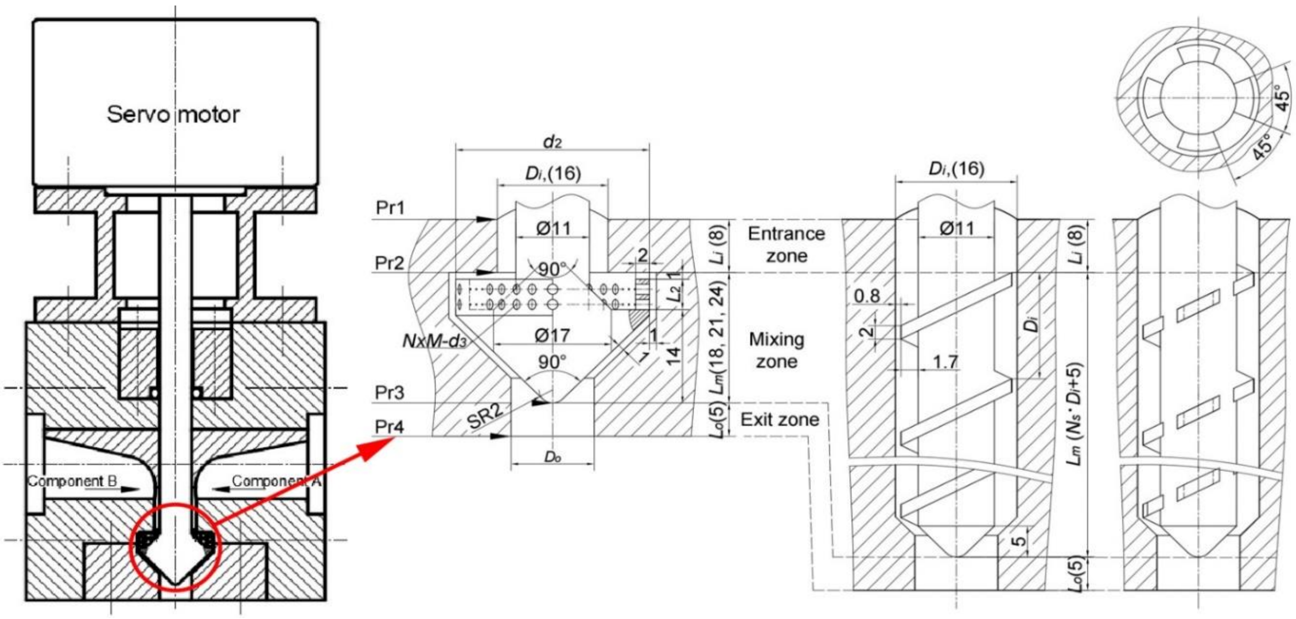

a b c d

Fig. 1 Mixers: a) assembly drawing of dynamic mixer; b) the detail view of dynamic mixer; c) screw-based mixer; d) slotted-screw mixer

The models of the melts and the rotating parts in mixers are modeled using Solidworks software. The regular tetrahedral unstructured grids with edge length of 0.5 mm are meshed using Workbench software [13], as shown in Fig. 2. The grid overlapping technology is used to deal with the relationship between grids of melt and rotating parts [14].

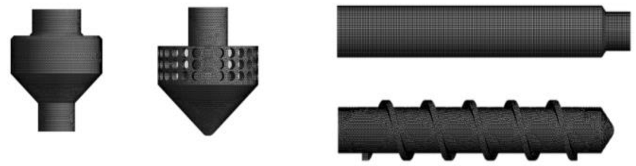

a b

Fig. 2 The grids of melts and rotating parts of mixers: a) the dynamic mixer; b) screw-based mixer

2.2. Governing equations and boundary conditions

The following assumptions are imposed on the current problem. The melt flow is a stable laminar flow of incompressible non-Newtonian fluid, ignoring inertia force, gravity, and effects of inlet and outlet, without wall slip behavior, and fully filling the channel [15]. Based on the assumptions, the continuity, momentum, heat transfer and constitutive equations of the simulation are cited from the literature [16]. The relationships of viscosity and shear rate, moreover of viscosity and temperature are described by Bird-Carreau model and Arrhenius model [17]. And the physical parameters used in the simulation are from literatures [18, 19].

The boundary conditions include: The inlet flow rate is 15, 30 and 45 mL/min, and the pressure of outlet is 0.1 MPa. The melt temperatures of the inlet and channel wall are constant, both 200 °C. The rotational speed of rotor is set as 60, 120, 180, 240, and 300 r/min. In the Taguchi orthogonal arrays method, the inlet flow rate is 30 mL/min, and rotor rotational speed is 240 r/min.

2.3. Calculation and result characterization

The current problem is calculated using the Polyflow software, with a convergence accuracy 10^{-5} [20]. The Δp is calculated as follows:

$$\Delta p = |p_i - p_0|, \tag{1}$$

where: p_i is the inlet pressure, and p_o is the outlet pressure.

In order to characterize the melt mixing quality, the 1000 tracer particles with different colours are added at the left and right sides of the inlet of the mixers, as shown in Fig. 3.

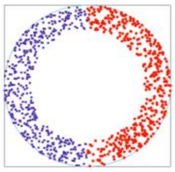

Fig. 3 Distribution of tracer particles at the inlet of mixer

The S named as segregation scale, is calculated using Eqs. (2)-(4) [9].

$$S = \int_0^{\xi} \left(R|r|\right) d\left(|r|\right), \tag{2}$$

$$R|r| = \frac{\sum_{j=1}^{n} \left(C'_j - \bar{C}\right)\left(C''_j - \bar{C}\right)}{n\sigma^2}, \tag{3}$$

$$\sigma^2 = \frac{\sum_{i=1}^{2m} C_i - \bar{C}}{2m-1}, \tag{4}$$

where: C'_j and C''_j are particle concentrations of two positions with a distance r from each other; $\bar{C}$ is average particle concentration; C_i is particle concentration at any point. n is the number of particle pairs; m is the number of particles; σ^2 is the variance of the particle concentration.

2.4. Taguchi orthogonal arrays method and results analysis

Taguchi orthogonal arrays method L9(3^4) [21] with three parameters N, M, d_3 and three levels (as shown in Table 1) are designed to optimize the dynamic mixer. The effects of parameters on the responses S, Δp and $S \cdot \Delta p$ are analysed using Range analysis and Analysis of Variance (ANOVA). Based on the most effective structure for the minimum $S \cdot \Delta p$, the influences of the flow rate and rotational speed on S and Δp of dynamic mixer are further studied, and compared with those of screw-based mixer and slotted-screw mixer.

3. Result and discussion

3. 1. The results of Taguchi orthogonal arrays method

The results of Taguchi orthogonal arrays method are showed in Table 2. From the perspective of melt mixing quality and energy consumption, the criterion that "the smaller, the better" is used to evaluate S, Δp and $S \cdot \Delta p$.

The results of Range analysis are showed in Table 3. For S, the N has the largest R of 72.13 µm, then the M has 22.00 µm, and at last the d_3 has the smallest R of 20.53 µm, So the influencing order for S is $N > M > d_3$. Similarly, it can be concluded that the influencing order for Δp is $d_3 > N > M$, and the influencing order for $S \cdot \Delta p$ is $N > d_3 > M$.

The influencing trends of parameters on the three responses are showed in Fig. 4. It is observed that the larger the N, M and d_3, S is minimizing, meaning the mixing uniformity can be increased. The similar influencing trends are observed about N, M, and d_3 on the $S \cdot \Delta p$. Therefore, it can be determined that the most effective parameters for the minimum S and $S \cdot \Delta p$ are N3 M3 $d_3$3 (i. e. N=3, M=26 and d_3=2.5 mm). With above parameters, S of 12.11 µm and $S \cdot \Delta p$ of 27.61 µm·MPa are obtained in a new test. They are the minimum in all the tests.

Table 2

L9 (3^4) Taguchi orthogonal arrays method scheme and results

Test serial number	Factor			Test results		
	N	M	d_3	S, µm	Δp, MPa	$S \cdot \Delta p$, µm·MPa
1	1	1	1	138.2	2.398	331.4
2	1	2	2	119.3	2.361	281.6
3	1	3	3	105.6	2.265	239.2
4	2	1	2	76.30	2.531	193.1
5	2	2	3	58.20	2.289	133.2
6	2	3	1	68.80	2.667	183.5
7	3	1	3	51.40	2.428	124.8
8	3	2	1	69.80	2.616	182.6
9	3	3	2	25.50	2.404	61.30
The most effective for Δp	1	2	3	113.3	2.220	251.5
The most effective for S and $S \cdot \Delta p$	3	3	3	12.11	2.280	27.61

Table 3

The results of range analysis

		N	M	d_3
S, µm	k_1	121.0	88.63	92.27
	k_2	67.77	82.43	73.70
	k_3	48.90	66.63	71.73
	R	72.13	22.00	20.53
	Influencing order	I	II	III
The most effective factors for S		N3 M3 $d_3$3		
Δp, MPa	k_1	2.341	2.452	2.560
	k_2	2.496	2.422	2.432
	k_3	2.483	2.445	2.327
	R	0.154	0.031	0.233
	Influencing order	II	III	I
The most effective factors for Δp		N1 M2 $d_3$3		
$S \cdot \Delta p$, µm·MPa	k_1	284.1	216.4	232.5
	k_2	169.9	199.2	178.7
	k_3	122.9	161.3	165.7
	R	161.2	55.10	66.80
	Influencing order	I	III	II
The most effective factors for $S \cdot \Delta p$		N3 M3 $d_3$3		

However, the influencing trends of three factors on Δp are complicated. The Δp firstly increases then decreases with the increase of N, but firstly decreases then augments with the growing M, and monotonously reduces with the decreasing d_3. According to the criteria that the smaller the better and Fig. 4, b, the most effective parameters for the minimum Δp are N1 M2 $d_3$3 (i. e. N=1, M=20 and d_3=2.5 mm), and the corresponding Δp of 2.22 MPa is obtained in a new test with these parameters. It is also the smallest one in all the tests.

Finally, the most effective structure for S and $S \cdot \Delta p$ is selected to further study its mixing properties.

The results of ANOVA and significant levels are shown in Table 4. For S, the F-values of N, M and d_3, are 56.12, 5.160 and 5.148, respectively. According to the criteria that if the F-value is smaller than 19, the corresponding parameter is an insignificant one, that if the F-value ranges between 19 and 99, the corresponding parameter is a significant one with level *, and that if the F-value is larger than 99, the corresponding parameter is a significant one with level **[22], both the F-values of M and d_3 are less than 19. So the N is the most significant parameter with level *, and both the M and d_3 are not significant factors for S.

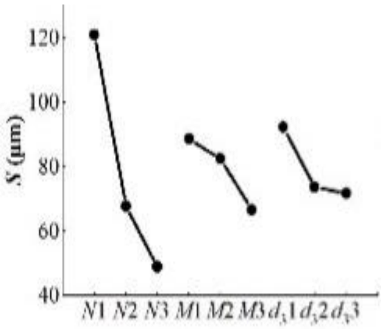

a

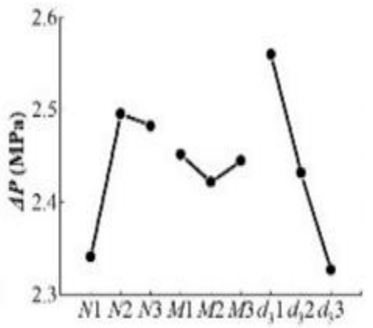

b

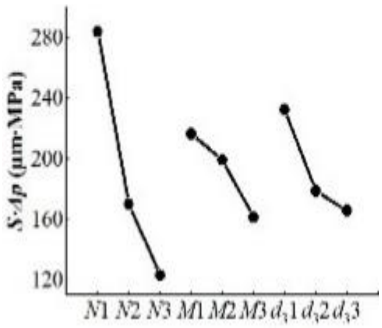

c

Fig. 4 Influencing trend of various factors on the three responses: a) S; b) Δp; c) $S{\cdot}\Delta p$

For Δp, the d_3 has the largest F-values of 3.092, then followed by N, and the M has the smallest one. They are all less than 19, so all the three factors are insignificant for Δp.

Moreover, for $S{\cdot}\Delta p$, the N has the largest F-values of 29.38, then followed by d_3, and the M has the smallest one of 3.402. So, the N is the most significant parameter with a level *, and both the M and d_3 are not significant factors for $S{\cdot}\Delta p$. The result is similar with the result of ANOVA for S.

In addition, the significant orders of three factors for three responses from ANOVA are all same with the influencing order from Range analysis. It is illustrated that both the results of Range analysis and ANOVA are reliable.

Table 4

The results of ANOVA

	Source	df	F- critical value	Adj. SS	F-value	Level of significance
S	N	2	19(*), 99(**)	8.397	56.12	*
	M	2		0.772	5.160	—
	d_3	2		0.770	5.148	—
	Error	2		0.150	—	—
	Total	8		10.09	—	—
Δp	N	2		44.05	1.669	—
	M	2		1.522	0.05767	—
	d_3	2		81.61	3.092	—
	Error	2		26.39	—	—
	Total	8		153.6	—	—
$S{\cdot}\Delta p$	N	2		41.21	29.38	*
	M	2		4.772	3.402	—
	d_3	2		7.520	5.361	—
	Error	2		1.403	—	—
	Total	8		54.91	—	—

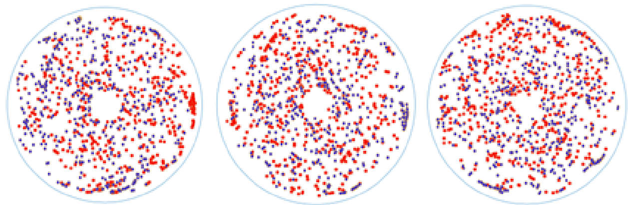

a b c

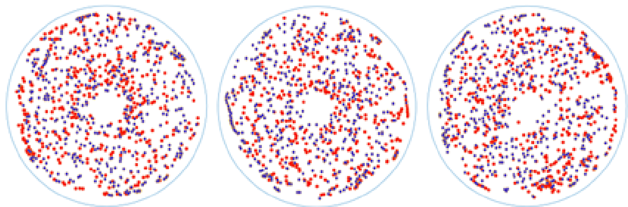

d e f

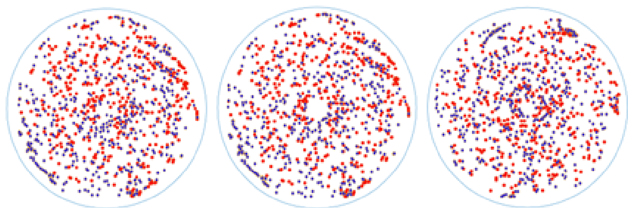

g h i

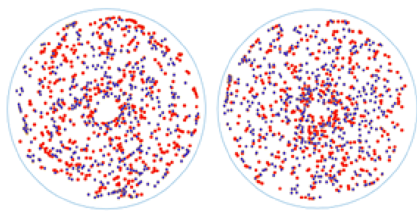

j k

Fig. 5 Distribution of tracer particles at the outlet surface of dynamic mixers: a) to i) Test 1 to 9; j) the most effective structure for Δp; k) the most effective structure for S and $S{\cdot}\Delta p$)

Fig. 5 shows the distributions of tracer particles at the outlet surface of dynamic mixers. It can be found that the distribution of tracer particles in the dynamic mixer with the most effective structure is the most uniform in 11 tests.

The agglomeration of particles is seldom found in the most effective structure for S and $S{\cdot}\Delta p$, as shown in Fig. 5, k. However, some agglomerations of particles are observed in the other tests. Especially in Test 1 (shown as in Fig. 5, a), there are some agglomerations with size of 0.77 mm.

From Table 1, it is found that the test 1 has the smallest N, M and d_3, and the most effective structure for S and $S{\cdot}\Delta p$ has the largest N, M and d_3. So, the results in Fig. 5 once again validate the conclusion that the larger N, M and d_3 are, the smaller S is, which is based on the Range analysis.

3. 2. The melt mixing quality of dynamic mixer

As can be seen from Fig. 6, the distribution of tracer particles on the cross section gradually becomes uniform from the inlet to the outlet. The slightly mixed red and blue particles are observed on the position Pr2. It is due to that there is axial and circumferential velocity (as shown in Fig. 7). The former is from the melt flow, and the latter is from rotational shaft in the entrance zone. And because the wall of channel is stationary, there is a velocity difference between the melt zones near to rotor and near to wall. The velocity differences in the two directions are small, but can make the particles move relatively, so the red and blue particles are slightly mixed.

In the mixing zone, there are not only the velocity differences in circumferential and axial directions, but also the velocity difference in radial velocity (as shown in Fig. 7). It is because that the part of melt is hindered by skirt, and divert to pass through the gap or holes nearby, however, the other part directly goes through the holes on the skirt. It leads to a large velocity difference in radial direction, and strengthen the mixing in axial direction. Therefore, the more uniform particle distribution can be obtained at the outlet of mixing zone (i. e. the position of Pr3).

In the exit zone without moving part, the melt flows in the form of a cylinder. There is only velocity difference in axial direction due to the stationary wall and flowing melt (as shown in Fig. 7). So, the melt mixing quality of exit zone is the smallest among the three zones of dynamic mixer. Due to this reason, the particles distribution in Fig. 6, c and d are similar, and some slight anti-mixing phenomena are observed, especially in the center of Fig. 6, d.

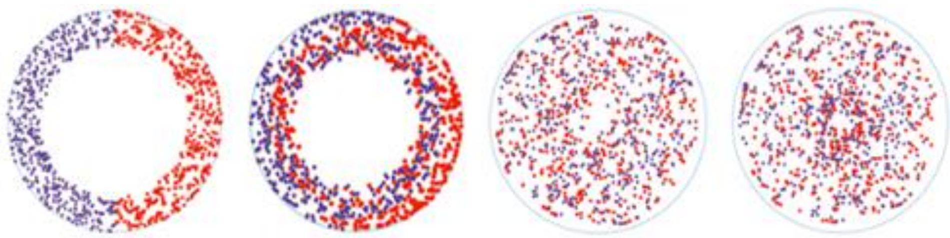

a b c d

Fig. 6 Distribution of tracer particles along the flow direction in the most effective dynamic mixer: a to d – the positions of Pr1 to Pr4

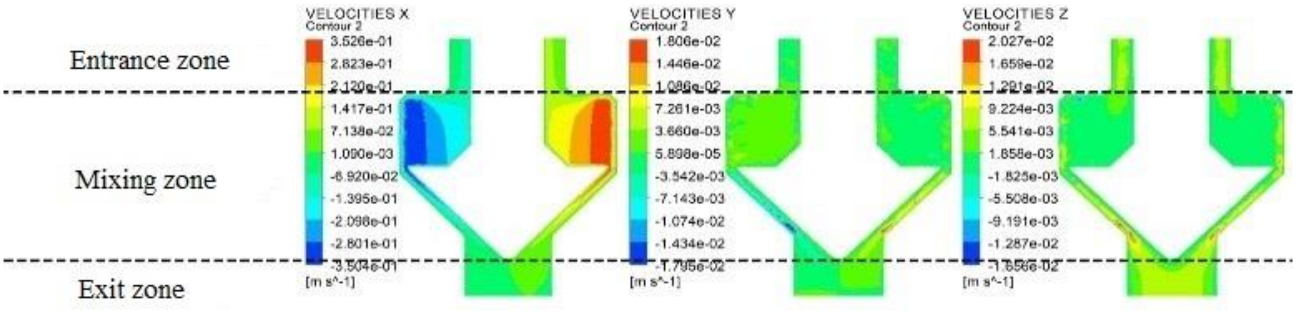

a b c

Fig. 7 The distribution of velocity components: a) axial; b) circumferential; c) radial direction

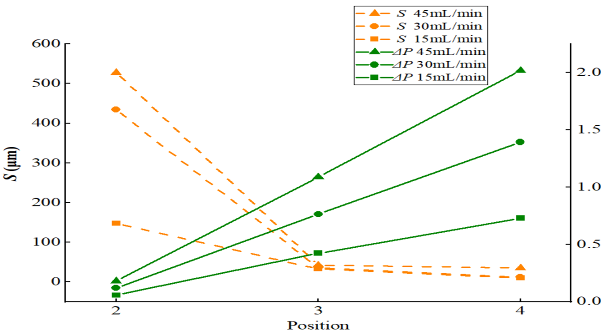

Fig. 8 The S and Δp at different observation positions

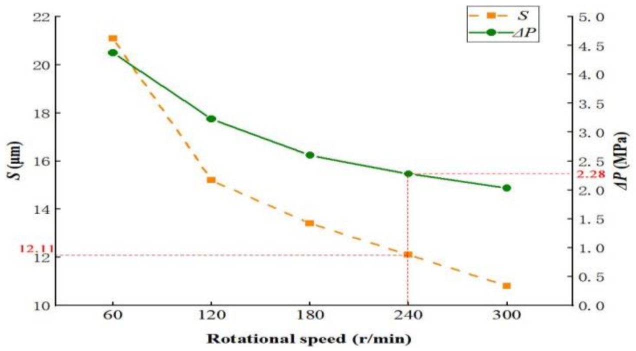

Fig. 9 The changes of S and Δp with rotational speed of the rotor (the flow rate of 30 mL/min)

From the Fig. 8, it can be observed that the decline of S is the largest while the melt flows through the mixing zone. This result is consistent with the above analysis. In addition, it is also found that the increase of flow rate leads to an increase of S and Δp. When the flow rate increases from 15 to 30 and 45 mL/min, the corresponding S changes from 10.1 to 12.11 and 35.2 μm, with increase by 19.9% and 248.5%, and the corresponding Δp increases from 1.31 to 2.38 and 3.4 MPa, with increase 81.68% and 159.5%. So, it can be concluded that the larger flow rate results in the less uniform mixing and the larger pressure drop in the dynamic mixer. This may be because that the larger flow rate reduces the residence time of the melt in dynamic mixer, which weakens the effects of rotor on the melts, so the melt mixing is less uniform. On the other hand, the Δp increases with the increment of axial velocity component resulted from the flow rate augment.

A significant decrease of Δp is also observed with the augment of rotational speed. The Δp decreases by 53.5%, from 4.37 to 2.03 MPa, while increasing the rotational speed from 60 to 300 r/min. This may be due to that the larger rotational speed leads to the larger shear rate, which results in a decrease in melt viscosity, as shown in Fig. 10. The maximum shear rate increases from 116.7 to 584.6 s^{-1}, and the corresponding melt viscosity reduces by 39.2% from 4422.5 to 2688.1 Pa·s, while rotational speed increasing from 60 to 300 r/min. The reduction of melt viscosity makes it flow easily. Therefore, the required Δp decreases while increasing the rotational speed of the rotor.

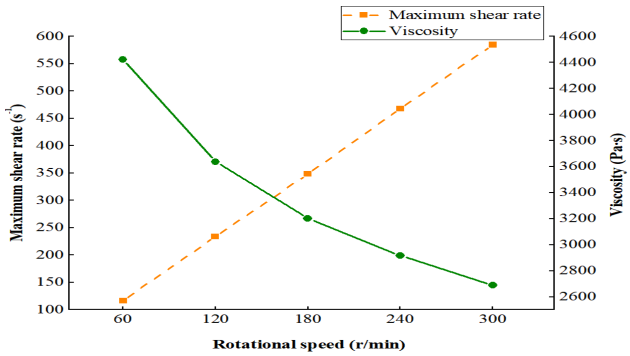

Fig. 10 The changes of maximum shear rate and melt viscosity with the rotational speed of the rotor (the flow rate of 30 mL/min)

3. 3. Comparison with screw-based mixers

Form Fig. 11, it can be observed that the S decreases while Δp increases with the augment of the length of the screw-based mixer and slotted-screw mixer. In addition, it is also observed that both the S and Δp increase with an increasing flow rate from 15 to 45 mL/min.

In order to achieve the same S of 12.11 μm obtained by dynamic mixer with the flow rate 30 mL/min and rotational speed 240 r/min, the total length of 98 mm and 95 mm (about $6{\cdot}D_i$) are required for screw-based mixer and slotted-screw mixer, respectively. Their total length (37 mm) is about 2.6 times as much as that of dynamic mixer. And the corresponding Δp of the screw-based mixer and slotted-screw mixer are 5.38 and 1.79 MPa. The Δp of the former is about 2.36 times as much as that of dynamic mixer, while the Δp of the latter is close to that of dynamic mixer. This may be due to that grooves in slotted-screw play the same role as holes in dynamic mixer, promoting melt mixing quality and reducing flow resistance by increasing flow space.

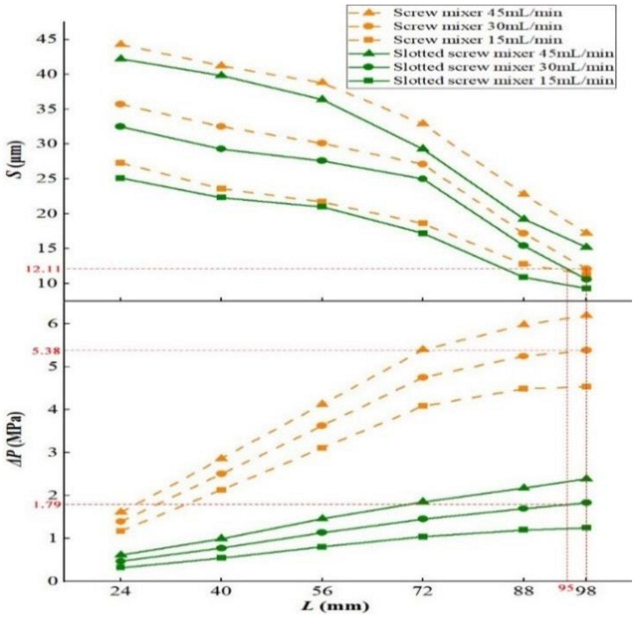

Fig. 11 The changes of S and Δp with the total length (rotational speed is 240 r/min)

Similar to dynamic mixer, the S of two types screw-based mixers substantially decrease with the rotational speed increasing, as shown in Fig. 12. But the changes of the Δp of two types screws are different. The Δp of slotted-screw mixer has a larger reduction with increasing rotational speed, that is similar to dynamic mixer. However, Δp of screw-based mixer has a small reduction with the rotational speed increasing, which is obviously different from dynamic mixer. It is indicated again that the dynamic mixer and slotted mixer have the similar mixing properties, that both the S and Δp substantially decreases with the rotational speed increasing. From the changing the S and Δp with the rotational speed, it is again illustrated that the holes of dynamic mixer and the grooves of slotted-screw mixer play the similar function.

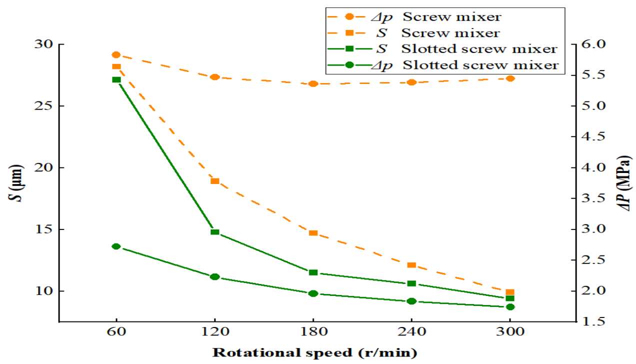

Fig. 12 The changes of S and Δp with the rotational speed (flow rate is 30 mL/min)

4. Conclusion

In this study, the structure parameters N, M and d_3 of mixing zone are selected to investigated their influences on the segregation scale S and pressure drop Δp of dynamic mixer, and the most effective structure for the minimum $S{\cdot}\Delta p$ are obtained through Taguchi orthogonal arrays method. Moreover, the melt mixing quality of dynamic mixer is compared with that of screw-based and slotted-screw mixers. The main conclusions include as following:

1. The melt mixing process is mainly carried out in the mixing zone of dynamic mixer. The larger the parameters N, M, d_3 are, the smaller the S will be (i. e. the mixing uniformity can be increased). In three parameters, the most significant one for S and $S{\cdot}\Delta p$ is N, and that for Δp is d_3. The most effective structure parameters N, M and d_3 for the minimum S and $S{\cdot}\Delta p$ are 3, 26 and 2.5 mm, respectively.

2. In the most effective dynamic mixer, the S increases with the flow rate increasing, and decreases with the rotational speed increasing. When rotational speed is 240 r/min, the increment of flow rate from 15 to 45 mL/min leads to the 248.5% increase of the S. While the flow rate is 30 mL/min, the increment of rotational speed from 60 to 300 r/min leads to the 48.8% drop of the S. While the flow rate is 30 mL/min and rotational speed is 240 r/min, the S is 12.11 μm.

3. In the most effective dynamic mixer, the Δp increases with the flow rate increasing, and decrease with the rotational speed increasing. When rotational speed is 240 r/min, the increment of flow rate from 15 to 45 mL/min leads to the 159.5% increase of the Δp. While the flow rate is 30 mL/min, the increment of rotational speed from 60 to 300 r/min leads to the 53.5% drop of the Δp. While the flow rate is 30 mL/min and rotational speed is 240 r/min, the Δp is 2.28 MPa.

4. The dynamic mixer requires shorter length and lower pressure drop to obtain uniform mixing than the screw-based mixers. To achieve the same mixing quality, (i. e. the S is 12.11 μm), the needed total lengths of the screw-based and slotted-screw mixer are about 2.6 times that of the dynamic mixer. Both the Δp of dynamic mixer and slotted-screw mixer significantly decreased with the rotational speed increasing from 60 to 300 r/min, while the Δp of screw-based mixer changes slightly with rotational speed increasing.

References

1. **Eriksson, M.; Meuwissen, M.; Peijs, T.; Goossens, H.** 2020. The Influence of melt-mixing conditions and state of dispersion on crystallisation, rheology and mechanical properties of PCL/Sepiolite nanocomposites, International Polymer Processing 35(3): 302-313. https://dx.doi.org/10.3139/217.3890.
2. **Hannes, B.; Johannes, K.** 2022. Detecting mixing barriers in Twin-Screw extruder elements via Lagrangian Coherent Structures, Chemical Engineering Science 263. https://dx.doi.org/10.1016/j.ces.2022.118069.
3. **Lv, Y.; Ye, C. L.; Zhang, J. L.; Guo, C. L.** 2019. Rapid and efficient synthesis of highly crystalline SSZ-13 zeolite by applying high shear mixing in the aging process, Microporous and Mesoporous Materials 293. https://dx.doi.org/10.1016/j.micromeso.2019.109812.
4. **Mahmoodi, H.; Razzaghi, K.; Shahraki, F.** 2020. Improving mixing performance by curved-blade static mixer, AIChE Journal 66(11). https://dx.doi.org/10.1002/aic.17034.
5. **Robinson, M.; Cleary, P. W.** 2019. Effect of geometry and fill level on the transport and mixing behaviour of a co-rotating twin screw extruder, Computational Particle Mechanics 6(2): 227-247. https://dx.doi.org/10.1007/s40571-018-0210-y.
6. **Cai, R. H.; Hou, Z. C.; Zhao, Y. Z.** 2019. Numerical study on particle mixing in a double-screw conical mixer, Powder Technology 352: 193-208. https://dx.doi.org/10.1016/j.powtec.2019.04.065.
7. **Belhout, C.; Bouzit, M.; Menacer, B.; Kamla, Y.** 2020. Numerical study of viscous fluid flows in a kenics static mixer, Mechanika 26(3): 206-211. http://dx.doi.org/10.5755/j01.mech.26.3.24160.
8. **Huo, C. F.; Feng, P.; Fan, C. G.; Lin, W. G.; Song, W. L.** 2016. Characterization of transverse mixing in a screw mixer by image analysis, Drying Technology an International Journal 34(2): 194-205. https://dx.doi.org/10.1080/07373937.2015.1036285.
9. **Connelly, R. K.; Kokini, J. L.** 2007. Examination of the mixing ability of single and twin screw mixers using 2D finite element method simulation with particle tracking, Journal of Food Engineering 79(3): 956–969. https://dx.doi.org/10.1016/j.jfoodeng.2006.03.017.
10. **Abdelghani, B.; Mohamed, B.** 2019. Numerical investigation of hydrodynamics induced by a pitched blade turbine: effect of the shape of vessel base, Mechanika 25(5): 370-376. https://dx.doi.org/10.5755/j01.mech.25.5.23015.
11. **Talhaoui, A.; Draoui, B.; Youcefi. A.** 2021. Effect of geometry design on mixing performance of newtonian fluid using helical overlapped mixer elements in kenics static mixer, Journal of Applied Fluid Mechanics 14(6): 1643-1656. https://dx.doi.org/10.47176/jafm.14.06.32494.
12. **Marschik, C.; Osswald, T. A.; Roland, W.; Albrecht, H.; Skrabala, O.; Miethlinger, J.** 2019. Numerical analysis of mixing in block-head mixing screws, Polymer Engineering and Science 59: E88-E104. https://dx.doi.org/10.1002/pen.24968.
13. **Sun, D. X; Wang, W. Y; Ju, Y. F.** 2021. Shearing and mixing performance of ultrahigh-molecular-weight hydrolyzed polyacrylamide (HPAM) solution in a helixes static mixer, Tehnički vjesnik 28(2): 465-472. https://dx.doi.org/10.17559/TV-20190712015659.
14. **Maureen, L. R.; Jozef, L. K.** 2013. Effect of mixer geometry and operating conditions on mixing efficiency of a non-Newtonian fluid in a twin screw mixer, Journal of Food Engineering 118: 256-265. https://dx.doi.org/10.1016/j.jfoodeng.2013.04.020.
15. **Yu, Y. F.; Chen, Y. X.; Meng, H. B.** 2022. Numerical analysis of thermal dynamics and mixing performance in the blade-type static mixers, Journal of Mechanical Science and Technology 36(7): 3701-3716. https://dx.doi.org/10.1007/s12206-022-0644-2.
16. **Sun, D.; Zhu, X.; Gao, M.** 2019. 3D numerical simulation of reactive extrusion processes for preparing PP/TiO2 nanocomposites in a corotating twin screw extruder, Materials 12(4): 671. https://dx.doi.org/10.3390/ma12040671.
17. **Kajiwara, T.; Nagashima, Y.; Nakano, Y.** 2010. Numerical study of twin-screw extruders by three-dimensional flow analysis-development of analysis technique and evaluation of mixing performance for full flight screws, Polymer Engineering & Science 36(16). https://dx.doi.org/10.1002/pen.10611.
18. Ansys. 2019. POLYFLOW 19.1 User's Guide.

19. **Ishikawa, T.; Kihara, S.; Funatsu, K.** 2010. Numerical simulation and experimental verification of nonisothermal flow in counter-rotating nonintermeshing continuous mixers, Polymer Engineering & Science 40(2): 365-375.
https://dx.doi.org/10.1002/pen.11170.
20. **Fu, H. L.; Ma, L. J.; Wang, H. Y.** 2018. Experimental and numerical studies of residence time in SK direct contact heat exchanger for heat pump, Chemical Engineering Research and Design.
https://dx.doi.org/10.1016/j.cherd.2018.05.013.
21. **Wang, Q.; Yang, C.; Du, K.** 2019. Effect of micro injection molding parameters on cavity pressure and temperature assisted by Taguchi method, Mechanika 25(4): 261-268.
http://dx.doi.org/10.5755/j01.mech.25.4.20999.
22. **Nourbakhsh, M.; Mashinchi, M.; Parchami, A.** 2013. Analysis of variance based on fuzzy observations, International Journal of Systems Science 44(4-6): 714-726.
https://dx.doi.org/10.1080/00207721.2011.618640.

J. Sun, J. Wang, Y. Zheng, Z. Li

TUNING OF MIXING ZONE PARAMETERS IN A DYNAMIC MIXER AND PERFORMANCE COMPARISON WITH SCREW-BASED MIXERS

S u m m a r y

A new dynamic mixer has been designed for the mixing of two polymer melts. Three main design parameters (number of circles of holes *N*, number of holes *M* per circle, and diameter of the holes d_3) for the mixing zone of the dynamic mixer were selected to study their influences on the pressure drop Δp and the segregation scale *S* using Taguchi orthogonal arrays method. The influences of flow rate and rotational speed were also investigated. In addition, the melt mixing quality was compared with that of screw-based and slotted-screw mixers. The results showed that the most significant factor influencing *S* and $S{\cdot}\Delta p$ is *N*. Both Δp and *S* increased with increasing flow rate, and decreased with increasing rotational speed. Compared to the screw-based and slotted-screw mixers, the dynamic mixer had a uniform melt mixing quality and shorter length.

Keywords: dynamic mixer, screw-based mixer, numerical simulation, segregation scale, Taguchi orthogonal arrays method.

Received January 15, 2023
Accepted August 2, 2023